Hindawi Publishing Corporation
Journal of Theoretical Chemistry
Volume 2014, Article ID 680987, 13 pages
http://dx.doi.org/10.1155/2014/680987

Research Article

Isolation, Identification, Molecular and Electronic Structure, Vibrational Spectroscopic Investigation, and Anti-HIV-1 Activity of Karanjin Using Density Functional Theory

Anoop kumar Pandey,[1] Abhishek Kumar Bajpai,[2] Ashok Kumar,[3] Mahesh Pal,[4] Vikas Baboo,[3] and Apoorva Dwivedi[2]

[1] *Department of Physics, Government Danteshwari P.G.College, Dantewada 494449, India*
[2] *Department of Physics, Government Kakatiya Post Graduate College, Jagdalpur, Bastar, Chhattisgarh 494001, India*
[3] *Department of Chemistry, Lucknow University, Lucknow 226007, India*
[4] *National Botanical Research Institute, Lucknow 226007, India*

Correspondence should be addressed to Apoorva Dwivedi; apoorvahri@gmail.com

Received 17 January 2014; Revised 9 April 2014; Accepted 9 April 2014; Published 7 May 2014

Academic Editor: Hugo Verli

"Karanjin" (3-methoxy furano-2,3,7,8-flavone) is an anti-HIV drug, and it is particularly effective in the treatment of gastric problems. The method of isolation of "Karanjin" followed the Principles of Green Chemistry (eco-friendly and effortless method). The optimized geometry of the "Karanjin" molecule has been determined by the method of density functional theory (DFT). Using this optimized structure, we have calculated the infrared wavenumbers and compared them with the experimental data. The calculated wavenumbers are in an excellent agreement with the experimental values. On the basis of fully optimized ground-state structure, TDDFT//B3LYP/LANL2DZ calculations have been used to determine the low-lying excited states of Karanjin. Based on these results, we have discussed the correlation between the vibrational modes and the crystalline structure of "Karanjin." A complete assignment is provided for the observed FTIR spectra. This is the first report of the isolation, molecular and electronic structure using vibrational spectroscopic investigation, density functional theory, and anti-HIV-1 activity of "Karanjin."

1. Introduction

Pongamia pinnata is a medium sized glabrous tree, found throughout Indian forests [1]. Different parts of this plant have been used as a source of traditional medicine. *P. pinnata* seeds contain oil which is mainly used in tanning industry for dressing of leather and to some extent it is used in soap industry. Oil is employed in scabies, herpes, and leucoderma, and sometimes as stomachic and cholagogue in dyspepsia and sluggish liver [2]. "Karanjin" is an active principle responsible for the curative effects of the oil in skin disease [1]. Seed extract inhibits growth of herpes simplex virus and also possesses hypoglycemic, antioxidative, antiulcerogenic, anti-inflammatory, and analgesic properties [3]. During the course of exploration of new compounds from *P. pinnata* seed oil, several workers [4–6] have identified some new compounds of its seed oil apart from "Karanjin." "Karanjin" possess pesticidal [7], insecticidal [8], and anti-inflammatory activity [9].

Considering the role of "Karanjin" in different areas, in the present communication, we have carried out isolation and identification of "Karanjin" by ecofriendly method and tested for its anti-HIV activity. The molecular structure of the well-known natural product "Karanjin" has been studied using the density functional theory. The equilibrium geometry, harmonic vibrational frequencies, and HOMO-LUMO gap have been calculated by the density functional B3LYP method employing 6-311 G (d, p) as the basis set. The detailed interpretation of the vibrational spectra of Karanjin in terms of the normal mode analysis has been reported. The main objective of the present study is to investigate in detail the vibrational spectra of the important biological molecule (Karanjin) by DFT [10] method, which can presumably help

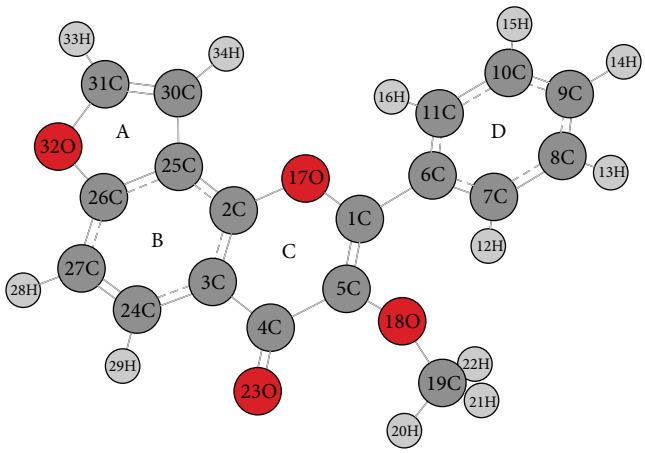

Figure 1: Model molecular structure of Karanjin.

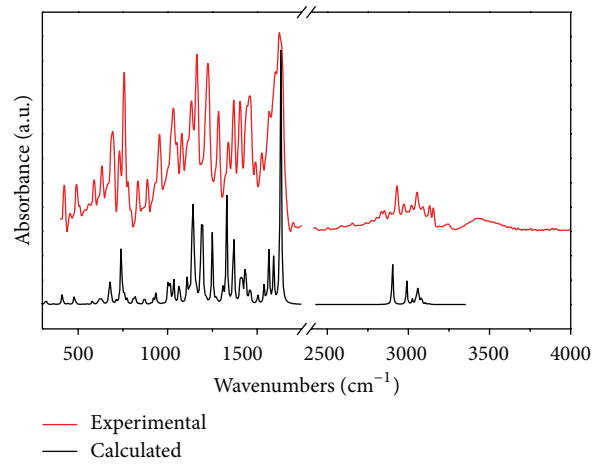

Figure 2: Comparison of calculated and experimental FTIR spectra of Karanjin.

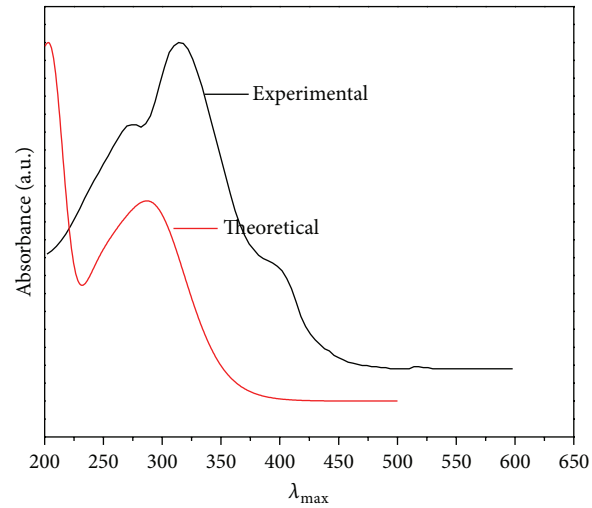

Figure 3: Comparison of calculated and experimental UV visible spectra of Karanjin.

in understanding its dynamical behavior. To the best of our knowledge, no detailed DFT calculations and anti-HIV activity have been performed on "Karanjin" so far in the literature.

2. Experimental Methods (Structure and Spectra)

The molecular structure of the title compound "Karanjin" is made by molecular modeling. The model molecular structure of the compound is given in Figure 1. Fourier transform infrared spectrum was recorded with FTIR Perkin Elmer spectrometer in KBr dispersion in the range of 500 to 4000 cm^{-1} for the title molecule. The comparison of the calculated and experimental FTIR and UV visible spectra of "Karanjin" is given in Figures 2 and 3, respectively.

3. Computational Methods

The initial geometry was generated from the standard geometrical parameters and was minimized without any constraint in the potential energy surface. The gradient corrected density functional theory (DFT) with the three-parameter hybrid functional (B3) [11] for the exchange part and the Lee-Yang-Parr (LYP) correlation function [12] has been employed for the computation of molecular structure, vibrational frequencies, HOMO-LUMO, and energies of the optimized structures, using Gaussian 09 [13]. The calculated vibrational frequencies have also been scaled by a factor of 0.963 [14]. By combining the results of the GaussView program [15] with symmetry considerations, vibrational frequency assignments were made with a high degree of accuracy. We used this approach for the prediction of IR frequencies of title compound and found it to be very straightforward. Density functional theory calculations are reported to provide excellent vibrational frequencies of organic compound if the calculated frequencies are scaled to compensate for the approximate treatment of electron correlation, for basis set deficiencies and for anharmonicity. A number of studies have been carried out regarding calculations of vibrational spectra by using B3LYP methods with 6-311 G (d, p) basis set. The scaling factor was applied successfully for B3LYP method and was found to be easily transferable in a number of molecules. Thus, vibrational frequencies calculated by using the B3LYP functional with 6-311G (d, p) as basis set can be utilized to eliminate the uncertainties in the fundamental assignment in the IR spectra.

4. Results and Discussion

4.1. Eco-Friendly Method. Here it needs to be highlighted that so far "Karanjin" has been isolated through column chromatography (silica gel, 100–200 mesh) or by preparative HPLC [16–18], but in our study the method was eco-friendly and effortless and followed the Principles of Green Chemistry. Implementing these Green Chemical Principles requires a certain investment, since the current, very inexpensive chemical processes must be redesigned. A typical chemical process generates products and wastes from raw

materials such as substrates, solvents, and reagents. If most of the reagents and the solvent can be recycled, the mass flow looks quite different.

4.2. Isolation of "Karanjin". The shade dried Karanja seeds (*Pongamia pinnata*) of 3.5 kg were extracted with methanol (MeOH) (4.5 lit) at room temperature. The combined MeOH extract was concentrated under reduced pressure at 40°C to a dark viscous mass. It was concentrated to dryness and kept at 4°C for 24 hr; after adding ethanol, shake it properly and keep on for settling down of crystals for few hours. Colorless crystals (11.2 g) were obtained from crystallization with EtOH isolated with TLC in 98 : 2 chloroform and MeOH and a single spot was obtained.

4.3. Identification of "Karanjin". Isolated compound identified as "Karanjin" (3-methoxy furano-(20,30 : 7,8)-flavone) by direct comparison of co-TLC and melting point of 162°C with that of authentic sample obtained from Sigma-Aldrich and was also confirmed by the ^{1}H NMR and ^{13}C NMR reported in the literature [19].

4.4. Cytotoxicity and Anti-HIV-1 Activity of Compound. Compound "Karanjin" was tested for cytotoxicity against C8166 cells (CC50), and anti-HIV-1 activity was evaluated by the inhibition assay for the cytopathic effects of HIV-1(EC_{50}) < using AZT as a positive control; the compound exerted moderate cytotoxic activity against C8166 cells with CC_{50} > 693.15 μM and showed anti-HIV-1 activity with EC_{50} = 49.43 μM and selectivity index (CC_{50}/EC_{50}) more than 14.02. Cytotoxicity and anti-HIV-1 activity of compound is shown in Table 1.

4.5. Anti-HIV-1 Assay. Cytotoxicity against C8166 cells (CC_{50}) was assessed using the MTT method, and anti-HIV-1 activity was evaluated by the inhibition assay for the cytopathic effects of HIV-1(EC_{50}) [20].

4.6. Molecular Structure. The equilibrium geometry optimization of "Karanjin" has been achieved by energy minimization, using DFT at the B3LYP level, employing LANL2DZ as the basis set given in Table 2. The optimized geometry of the molecule under study is confirmed to be located at the local true minima on potential energy surface, as the calculated vibrational spectra contain no imaginary wavenumber. "Karanjin" is an unsymmetrical molecule having C_1 point group symmetry. The given molecule has four rings. Out of these, three are six membered hexagonal rings and one five membered pentagonal ring in which A and C are heterocyclic rings in which one carbon is replaced by oxygen. Due to the antibonding repulsion, these rings are slightly shifted towards the plane. The given structure of "Karanjin" is slightly shifted from the planar structure to minimize its surface energy. Due to this reason, ring D gets shifted from its plane. The optimized bond length of C–C in five membered ring A ranges between 1.353 Å and 1.438 Å, while, for another six membered ring B, this ranges between 1.379 Å and 1.415 Å. The optimized bond length of C–C in six membered ring C ranges between 1.367 Å and 1.471 Å, while, for another six membered ring D, this ranges between 1.389 Å and 1.405 Å. This difference in the C–C bond length is attributed to the difference in bond strength. The optimized C–O bond lengths in ring A are found to be 1.362 Å and 1.373 Å, while, in ring C, the optimized C–O bond lengths are found to be 1.357 Å and 1.371 Å. The optimized C–O bond length attached to ring C is found to be 1.363 Å. Bond length of carbonyl group C=O attached to the ring C is calculated to be 1.227 Å. Values of all the bond angles are given in Table 2 and all are in agreement with the previous experimental and theoretical studies on different biomolecules [21–23].

Table 1

Compound	Cytotoxicity CC_{50} (μM)	Anti-HIV-1 activity, EC_{50} (μM)	Selectivity index, CC_{50}/EC_{50}
KJ	693.15	49.43	>14.02
AZT	5746.1	0.0147	390406.06

4.7. Vibrational Assignments. The molecule "Karanjin" contains 34 atoms and therefore has 96 normal modes of vibration. All the 96 fundamental vibrations are IR active. The harmonic vibrational frequencies calculated for Karanjin at DFT (B3LYP) level using LANL2DZ as the basis set and the experimental frequencies (FTIR) have been compared in Table 3 along with their vibrational assignments of the normal modes. Vibrational assignments are based on the observation of the animated modes in GaussView.

In "Karanjin," the C–H functional group is present at a number of positions. The stretching vibration, ν(C–H), is expected to occur in the region 2900–3200 cm^{-1}. The calculated values of the ν(C–H) vibration lie within this spectral range. For C–H stretching vibrations, intense bands are calculated at 2902, 2989, and 3060 cm^{-1} which matches well the experimental frequencies observed at 2929, 2972, and 3052 cm^{-1}.

The other important stretching vibrations correspond to the C=O moieties at the C_7 position. The region 1600–1750 cm^{-1} is generally considered as the double bond stretching region for C=O, C=C, and C=N bonds [24–27]. The C=O stretching vibration, ν(C=O), appears as a prominent mode in the FTIR spectra at 1624 cm^{-1} which matches well the calculated one, that is, 1632 cm^{-1}. For C–C stretching vibration an intense band is calculated at 1539 cm^{-1} which is found to be in good agreement with the experimental one, that is, 1526 cm^{-1}. Due to the deformation of ring A vibration, an intense band is calculated at 1369 cm^{-1} which is in very good agreement with the experimental one, that is, 1369 cm^{-1}. Due to breathing mode in ring B vibration, intense band is calculated at 1250 cm^{-1} which nearly matches the experimental one, that is, 1225 cm^{-1}. Due to out of plane (C–C–H) vibration, intense band appears at 739 cm^{-1}. The $-CH_3$ functional group is an important constituent of "Karanjin" and vibrations corresponding to this group are present in a number of modes. The stretching vibrations of these groups appear in a number of modes. An intense band due to butterfly motion in CH_3 appears in the experimental

Table 2: Optimized geometrical parameters of Karanjin by B3LYP/6-311G (d, p) methods.

S. number	Bond lengths	Calculated	Exp.	Bond angles	Calculated	Exp.
1	*R*(1, 2)	1.3795	1.363	*A*(2, 1, 6)	116.5065	116.5
2	*R*(1, 6)	1.3975	1.399	*A*(2, 1, 28)	122.364	—
3	*R*(1, 28)	1.0821	—	*A*(6, 1, 28)	121.1293	—
4	*R*(2, 3)	1.4157	1.403	*A*(1, 2, 3)	121.6696	121.6
5	*R*(2, 27)	1.0826	—	*A*(1, 2, 27)	121.4181	—
6	*R*(3, 4)	1.3939	1.384	*A*(3, 2, 27)	116.9123	—
7	*R*(3, 7)	1.4717	1.466	*A*(2, 3, 4)	120.0707	120.9
8	*R*(4, 5)	1.4039	1.411	*A*(2, 3, 7)	120.5299	121.4
9	*R*(4, 10)	1.3573	1.352	*A*(4, 3, 7)	119.3901	117.8
10	*R*(5, 6)	1.3991	1.374	*A*(3, 4, 5)	119.8451	118.8
11	*R*(5, 24)	1.4389	1.431	*A*(3, 4, 10)	122.4041	124.0
12	*R*(6, 26)	1.3621	1.355	*A*(5, 4, 10)	117.7498	117.2
13	*R*(7, 9)	1.4724	1.443	*A*(4, 5, 6)	117.6428	117.9
14	*R*(7, 11)	1.2273	1.238	*A*(4, 5, 24)	136.2417	135.7
15	*R*(8, 9)	1.3672	1.353	*A*(6, 5, 24)	106.1152	106.3
16	*R*(8, 10)	1.3712	1.366	*A*(1, 6, 5)	124.264	124.4
17	*R*(8, 13)	1.4743	1.474	*A*(1, 6, 26)	125.9683	125.1
18	*R*(9, 12)	1.3632	1.365	*A*(5, 6, 26)	109.7673	110.5
19	*R*(12, 31)	1.4406	1.454	*A*(3, 7, 9)	114.5711	115.3
20	*R*(13, 14)	1.4043	1.395	*A*(3, 7, 11)	122.8728	122.5
21	*R*(13, 18)	1.4055	1.389	*A*(9, 7, 11)	122.5555	122.1
22	*R*(14, 15)	1.391	1.388	*A*(9, 8, 10)	120.8623	120.9
23	*R*(14, 19)	1.0793	—	*A*(9, 8, 13)	127.8731	127.8
24	*R*(15, 16)	1.3929	1.390	*A*(10, 8, 13)	111.2639	111.3
25	*R*(15, 20)	1.0841	—	*A*(7, 9, 8)	121.7683	122.4
26	*R*(16, 17)	1.3936	1.367	*A*(7, 9, 12)	119.0806	117.7
27	*R*(16, 21)	1.0841	—	*A*(8, 9, 12)	119.0731	119.8
28	*R*(17, 18)	1.3894	1.388	*A*(4, 10, 8)	120.97	119.6
29	*R*(17, 22)	1.0842	—	*A*(9, 12, 31)	116.681	113.6
30	*R*(18, 23)	1.0818	—	*A*(8, 13, 14)	122.193	121.2
31	*R*(24, 25)	1.3531	1.335	*A*(8, 13, 18)	119.157	120.1
32	*R*(24, 29)	1.0773	—	*A*(14, 13, 18)	118.6442	118.7
33	*R*(25, 26)	1.3737	1.377	*A*(13, 14, 15)	120.2939	121.0
34	*R*(25, 30)	1.0771	—	*A*(13, 14, 19)	119.5231	—
35	*R*(31, 32)	1.0891	—	*A*(15, 14, 19)	120.1826	—
36	*R*(31, 33)	1.0884	—	*A*(14, 15, 16)	120.6002	119.1
37	*R*(31, 34)	1.0949	—	*A*(14, 15, 20)	119.3481	—
38	—	—	—	*A*(16, 15, 20)	120.051	—
39	—	—	—	*A*(15, 16, 17)	119.5338	120.1
40	—	—	—	*A*(15, 16, 21)	120.2524	—
41	—	—	—	*A*(17, 16, 21)	120.2136	—
42	—	—	—	*A*(16, 17, 18)	120.2358	120.9
43	—	—	—	*A*(16, 17, 22)	120.136	—
44	—	—	—	*A*(18, 17, 22)	119.6282	—
45	—	—	—	*A*(13, 18, 17)	120.6874	120.0
46	—	—	—	*A*(13, 18, 23)	119.4489	—
47	—	—	—	*A*(17, 18, 23)	119.8616	—
48	—	—	—	*A*(5, 24, 25)	105.5988	105.5
49	—	—	—	*A*(5, 24, 29)	127.7368	—
50	—	—	—	*A*(25, 24, 29)	126.6633	—
51	—	—	—	*A*(24, 25, 26)	112.0571	112.3

Table 2: Continued.

S. number	Bond lengths	Calculated	Exp.	Bond angles	Calculated	Exp.
52	—	—	—	A(24, 25, 30)	132.815	—
53	—	—	—	A(26, 25, 30)	115.1279	—
54	—	—	—	A(6, 26, 25)	106.4614	105.4
55	—	—	—	A(12, 31, 32)	105.499	—
56	—	—	—	A(12, 31, 33)	110.6157	—
57	—	—	—	A(12, 31, 34)	110.2584	—
58	—	—	—	A(32, 31, 33)	110.4607	—
59	—	—	—	A(32, 31, 34)	109.3804	—
60	—	—	—	A(33, 31, 34)	110.5095	—

Table 3: Vibrational assignments of Karanjin with B3LYP/6-311G (d, p).

B3LYP (calculate)	IR (int.)	Exp.	Vibrational assignments
41	0.4616	—	Ring D twist from rest of the molecule
47	0.0408	—	Slight bending in whole molecule
58	1.4783	—	Slight bending in whole molecule
71	1.2198	—	Rock CH_3
86	1.3868	—	Slight bending in whole molecule
99	1.2684	—	Twist CH_3
139	1.8339	—	Twist CH_3
165	0.5168	—	Twist CH_3
182	1.3627	—	Bending in whole molecule
216	3.8318	—	Floating of whole molecule
231	1.4454	—	Bending in whole molecule
257	4.7668	—	γ(C–C–C) in whole molecule
265	0.8668	—	Whole molecule stretching
299	1.2843	—	γ(C–C–C) in whole molecule
314	3.3777	—	Twist (C–O–CH_3)
324	4.4912	—	τ(C–C–C=O)
362	1.0152	—	τ(C–C–O–CH_3)
398	0.2783	—	γ(C–C–C) Ring D
412	16.6519	422	Ring A bends from joint to ring B
441	1.5627	—	γ(C–C–C) ring D
477	10.432	—	τ(C–C–C–C) in whole molecule
486	4.307	490	τ(C–C–O–CH_3)
525	0.5385	—	γ(C–C–H) rings A and B
549	1.0232	—	τ(C–C–C–C) ring B
580	5.7233	589	γ(C–C–H) ring A
607	1.0343	—	τ(C–C–C–C) ring D
615	5.088	—	τ(C–C–C–C) ring D
622	5.8291	—	τ(C–C–C–C) ring D
629	7.1766	632	γ(C–C–C) ring D + γ(C–C–H) ring D
639	2.7418	—	τ(C–C–C–O) + τ(C–C–C–C)
673	15.257	—	β(C–C–C) ring B
681	35.221	693	γ(C–C–H) ring D
714	5.4099	—	γ(C–C–H) ring A
739	70.1363	730	γ(C–C–H) ring A
743	19.7507	—	Bending in whole molecule
757	18.7847	757	γ(C–C–H) ring D + γ(C–C–C) ring D
773	7.1237	—	γ(C–C–H) in whole molecule

Table 3: Continued.

B3LYP (calculate)	IR (int.)	Exp.	Vibrational assignments
809	11.2216	—	γ(C–C–H) ring B
819	9.2691	—	β(C–C–C) ring B + β(C–O–C) ring A
825	1.1522	—	γ(C–C–H) ring D
839	0.8883	833	γ(C–C–H) ring A
870	12.1445	886	β(C–C–O) ring A + β(C–C–C) ring A
907	1.2768	—	γ(C–C–H) ring D
922	9.1487	—	β(C–C–C) rings C and D
935	16.2356	—	β(C–C–H) ring A + β(C–C–C) ring B
945	0.0615	—	γ(C–C–H) ring B
951	1.3957	954	γ(C–C–H) ring D
968	0.4403	—	γ(C–C–H) ring D
976	0.873	—	β(C–C–C) ring D
1002	24.0341	—	ω(O–H)
1006	14.4736	—	β(C–C–H) rings A and B + β(C–C–C) ring B
1014	24.7318	—	β(C–C–H) ring D
1034	37.6874	1032	β(C–C–O) ring A + β(C–C–H) ring A
1065	37.523	1078	β(C–C–H) ring D
1108	32.1303	—	β(C–C–H) rings A and B
1112	3.026	—	β(C–C–H) rings A and B
1120	14.9274	—	Twist CH_3
1138	3.8577	—	β(C–C–H) ring D
1140	195.8791	1132	β(C–C–H) in whole molecule + β(C–C–C) ring B
1151	51.793		Twist CH_3 + β(C–C–H) in whole molecule
1164	11.6598	1163	β(C–C–H) ring D
1187	103.9113	—	β(C–C–H) in whole molecule
1195	103.0799	—	β(C–C–H) ring B + twist CH_3
1214	5.214	—	β(C–C–H) rings A and B
1250	100.8387	1225	Breathing in ring B
1273	8.6432	—	Ring D deformation
1304	6.3433	—	β(C–C–H) ring D
1310	19.154	—	β(C–C–H) in whole molecule
1330	153.5339	1339	β(C–C–C) rings B and C + β(C–C–H) ring D
1369	121.7396	1369	Ring A deformation
1408	52.4486	1405	Butterfly in CH_3
1417	8.0248	—	β(C–C–H) in whole molecule
1418	17.7601	—	β(C–C–H) in whole molecule
1424	2.3616	—	S(H–C–H) in CH_3
1434	72.9917	—	β(C–C–H) ring B + ν(C–C) ring A
1456	17.1709	—	S(H–C–H) in CH_3
1465	14.0125	1460	β(C–C–H) ring D
1504	14.0743	—	ν(C–C) ring A
1539	26.0649	1526	ν(C–C) rings C and D
1554	6.2017	—	ν(C–C) in whole molecule
1566	74.9616	—	ν(C–C) in whole molecule
1578	1.1856	—	ν(C–C) ring D
1592	64.7197	—	Ring A deformation
1632	379.2331	1624	ν(C=O)
2902	62.4466	2929	ν(C–H) in (O–CH_3)
2989	35.857	2972	ν(C–H) in (O–CH_3)
3024	7.4574	—	ν(C–H) in (O–CH_3)

Table 3: Continued.

B3LYP (calculate)	IR (int.)	Exp.	Vibrational assignments
3038	0.0903	—	ν(C–H) ring D
3048	14.3705	—	ν(C–H) ring D
3060	29.321	3052	ν(C–H) ring D
3072	1.1549	—	ν(C–H) ring B
3078	5.8476	—	ν(C–H) ring D
3084	4.8586	—	ν(C–H) ring B
3106	2.4619	—	ν(C–H) ring D
3127	1.4105	3131	ν(C–H) ring A
3149	0.1629	3153	ν(C–H) ring A

ν: stretching; β: in plane bending; γ: out of plane bending; τ: torsion.

Table 4: Calculated parameters using TDDFT//B3LYP/LANL2DZ for Karanjin.

Excitation	CI coefficient	Expansion wave length (nm) calculated (Exp.)	Oscillator strength	Energy (eV)
Excited state 1				
74 → 77	0.29364	293.89 (310)	0.2818	4.2188
75 → 77	0.59270			
Excited state 2				
73 → 78	0.38454			
75 → 79	0.28540	209.02 (274)	0.3189	5.9317
76 → 81	0.35123			
Excited state 3				
69 → 78	0.29225			
70 → 79	0.37746	182.47	0.2131	6.7948
72 → 80	0.37599			

spectrum at 1405 cm^{-1} which matches well the peak at 1408 cm^{-1}, in the calculated spectrum.

In "Karanjin," a very important vibration corresponds to the modes involving the vibrations of the ring atoms. For the purpose of simplifying the analysis, we have classified the structure of "Karanjin" into four rings A, B, C, and D as shown in Figure 1. The ring stretching vibrations, ν (ring), are complicated combinations of the stretching of C–O and C–C bonds. The most important ring stretching vibrations are the ring breathing, ring deformation, and so forth. Other ring vibration modes present a mixed profile.

There are some frequencies in the lower region due to the torsion and mixed bending modes having appreciable IR intensity in calculated FTIR spectrum. Furthermore, the study of low frequency vibrations is of great significance, because it gives information on weak intermolecular interactions, which takes place in enzyme reactions [28]. Knowledge of low frequency mode is also essential for the interpretation of the effect of electromagnetic radiation on biological systems [29].

The calculated (scaled) and experimental frequencies show some deviation which can be due to the combination of electron correlation effects, insufficiency of basis set, and the unevenness of the potential energy surface and also may be explained by the presence of external medium taken during experimental FTIR analysis. The theoretical calculations have been done on gas-phase molecule.

4.8. Electronic Spectra and Electronic Properties of Karanjin. On the basis of fully optimized ground-state structure, TDDFT//B3LYP/LANL2DZ calculations have been used to determine the low-lying excited states of "Karanjin." The parameters calculated involve the vertical excitation energies, oscillator strength (f), and wavelength by using the Gaussian 09W code. Experimental wavelengths are not available so these calculated data can presumably help the experimentalists. Electronic transitions determined from excited state calculations are listed in Table 4 for the three lowest energy transitions of the molecule. TD-DFT calculation predicts three intense electronic transitions at 4.2188 eV (293.89 nm), 5.9317 eV (209.02), and 6.7948 eV (182.47) with an oscillator strengths of 0.2818, 0.3189, and 0.2131, respectively, which are compared with the measured experimental data (Exp. = 310 nm and 274 nm).

The electronic structure of the "Karanjin" in the gas phase has been calculated with DFT using the B3LYP /6-311 G (d, p) as the basis set. HOMO and LUMO are the basic electronic parameters associated with the orbital in a molecule and the difference between them, resulting in energy gap. Not only energy gap (frontier orbital gap) helps to describe the chemical reactivity and kinetic stability of the molecule but also these orbitals find out the way the molecule interacts with other species. The HOMO-LUMO energy gap is an important measure for stability index. It establishes correlations in various chemical and biochemical systems [30, 31].

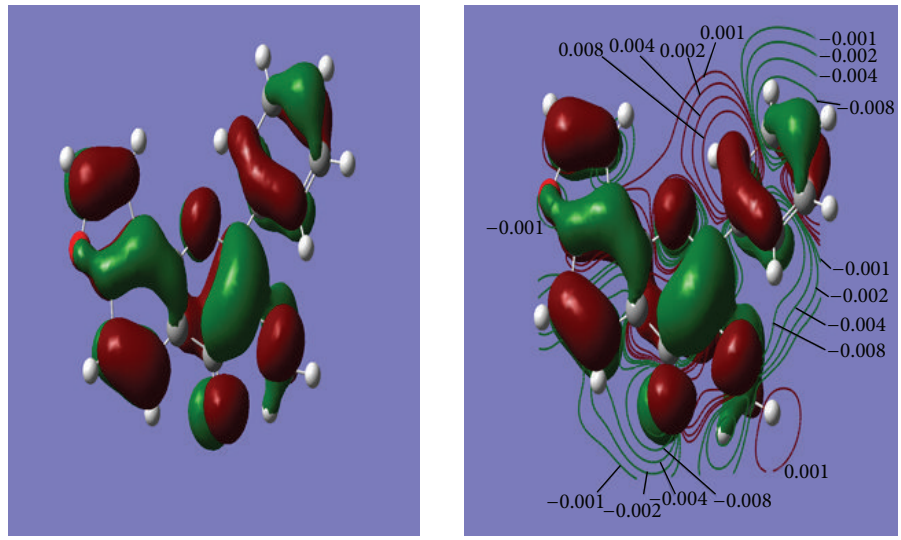

Figure 4: 3D and 2D plots of the highest occupied molecular orbital for Karanjin.

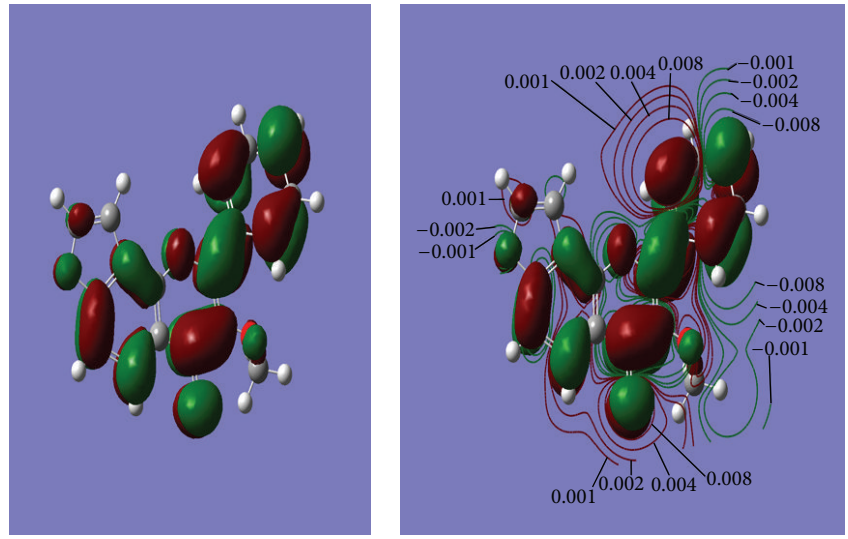

Figure 5: 3D and 2D plots of lowest unoccupied molecular orbital for Karanjin.

Table 5: Lowest energy, HOMO-LUMO gap (frontier orbital energy gap), and dipole moment of Karanjin by B3LYP/6-311G (d, p) methods.

Parameters	Karanjin
Energy (in au)	−994.2536
HOMO (in eV)	−6.17377
LUMO (in eV)	−1.92332
Frontier orbital energy gap (in eV)	4.25045
Dipole moment (in Debye)	3.86

The plots of the HOMO, LUMO, and electrostatic potential for both the molecules in 2D and 3D are shown in Figures 4, 5, and 6. The HOMO is found to be concentrated over the whole atoms, but the LUMO lies mainly over the whole molecule but less over ring A. The calculated value of the frontier orbital energy gap is 4.25 eV (Table 5). The low frontier orbital gap is also associated with a high chemical reactivity and low kinetic stability [32]. The molecular electrostatic potential (MESP) is an important factor by which we can confirm the electrostatic potential region distribution of size and shape of molecules as well as the total physiology of the molecules. We have plotted 2D and 3D MESP structures of the title compound as shown in Figure 6. The electronegative region is outside the molecule near the oxygen atoms. The energy equal to the shielded potential energy surface is required for any substitution reaction near oxygen. The electronegative lines (in between −0.08 a.u. and −0.02 a.u.) form a closed contour which clearly indicates that total flux passing in between these curves is not equal to zero. For any nucleophilic substitution reaction near oxygen (closed contour area), an amount of energy equal to shielded potential energy surface is required; however, remaining part of molecule is suitable for electrophilic substitution reaction. Thus, it can be

Table 6: Calculated ε_{HOMO}, ε_{LUMO}, energy band gap ($\varepsilon_L - \varepsilon_H$), chemical potential ($\mu$), electronegativity ($\chi$), global hardness ($\eta$), global softness ($S$), and global electrophilicity index (ω) for Karanjin at B3LYP/6-311G (d, p) level.

Karanjin	ε_H	ε_L	$\varepsilon_L - \varepsilon_H$	χ	μ	η	S	ω
A	−6.17377	−1.92332	4.25045	4.04854	−4.04854	2.12523	0.23527	3.85622

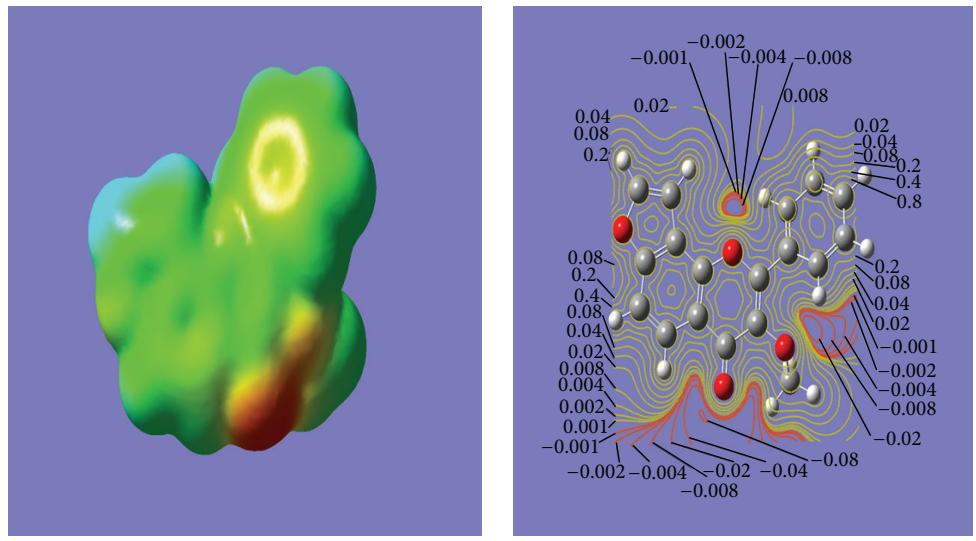

Figure 6: 3D and 2D plots of molecular electrostatic potential.

asserted that MESP values have been shown to be well related to biological properties [33–35].

4.9. Global Reactivity Descriptors. The energies of frontier molecular orbitals (ε_{HOMO}, ε_{LUMO}), energy band gap ($\varepsilon_{LUMO} - \varepsilon_{HOMO}$), electronegativity ($\chi$), chemical potential ($\mu$), global hardness ($\eta$), global softness ($S$), and global electrophilicity index (ω) [36–39] of "Karanjin" have been listed in Table 6. On the basis of ε_{HOMO} and ε_{LUMO}, these parameters are calculated using (1) as given below

$$\chi = -\frac{1}{2}\left(\varepsilon_{LUMO} + \varepsilon_{HOMO}\right)$$

$$\mu = -\chi = \frac{1}{2}\left(\varepsilon_{LUMO} + \varepsilon_{HOMO}\right)$$

$$\eta = \frac{1}{2}\left(\varepsilon_{LUMO} - \varepsilon_{HOMO}\right) \quad (1)$$

$$S = \frac{1}{2\eta}$$

$$\omega = \frac{\mu^2}{2\eta}.$$

4.10. Local Reactivity Descriptors. The Fukui function (FF) of a molecule provides information on the reactivity. The FF successfully predicts relative site reactivities for most chemical systems and as such it provides a method for understanding and categorizing chemical reactions. The atom with the highest FF value is highly reactive when compared to the other atoms in the molecule. These values represent the qualitative descriptors of reactivity of different atoms in the molecule. Ayers and Parr [40] have elucidated that molecules tend to react where the FF is the largest when attacked by soft reagents and in places where the FF is found to be smaller when attacked by hard reagents. The use of the Fukui functions for the site selectivity of the Karanjin molecule for nucleophilic and electrophilic attacks has been made with special emphasis to the dependence of the Fukui values on the basis of B3LYP/6-311G(d, p) level of theory. Using the Mulliken atomic charges of neutral, cation, and anion, state of Karanjin, the Fukui functions (f_k^+, f_k^-, f_k^0), local softness (s_k^+, s_k^-, s_k^0), and local electrophilicity indices ($\omega_k^+, \omega_k^-, \omega_k^0$) [37, 38], the Fukui functions are calculated using the following (2):

$$f_k^+ = \left[q(N+1) - q(N)\right] \quad \text{for nucleophilic attack}$$

$$f_k^- = \left[q(N) - q(N-1)\right] \quad \text{for electrophilic attack} \quad (2)$$

$$f_k^0 = \frac{1}{2}\left[q(N+1) + q(N-1)\right] \quad \text{for radical attack.}$$

Local softness and electrophilicity indices are calculated using (3)

$$s_k^+ = Sf_k^+, \qquad s_k^- = Sf_k^-, \qquad s_k^0 = Sf_k^0,$$
$$\omega_k^+ = \omega f_k^+, \qquad \omega_k^- = \omega f_k^-, \qquad \omega_k^- = \omega f_k^-, \quad (3)$$

where +, −, and 0 signs show nucleophilic, electrophilic, and radical attack, respectively.

The Fukui functions, local softnesses, and local electrophilicity indices for selected atomic sites in "Karanjin" have been listed in Table 7. The maximum values of all the three local electrophilic reactivity descriptors (f_k^+, s_k^+, ω_k^+) at C7 and

Table 7: (a) Fukui functions (f_k^+, f_k^-), local softnesses (s_k^+, s_k^-), and local electrophilicity indices (ω_k^+, ω_k^-) for selected atomic sites of Karanjin, using the Mulliken population analysis at B3LYP/6-311G (d, p) level. (b) (All atomic sites.)

(a)

Atom number	f_k^+	f_k^-	s_k^+	s_k^-	ω_k^+	ω_k^-
C1	−0.0098	0.09366	−0.0023	0.02203	−0.0377	0.36116
C2	0.09201	−0.0089	0.02165	−0.0021	0.35482	−0.0344
C7	0.09812	−0.0179	0.02309	−0.0042	0.37838	−0.0692
C14	0.02752	0.02195	0.00648	0.00516	0.10614	0.08463
C15	0.00421	0.02187	0.00099	0.00515	0.01623	0.08434
C16	0.06111	0.02641	0.01438	0.00621	0.23566	0.10185
C17	0.00646	0.01716	0.00152	0.00404	0.02491	0.06616
C18	0.044	0.01018	0.01035	0.0024	0.16969	0.03926
C24	−0.0138	0.05979	−0.0032	0.01407	−0.053	0.23054
C25	0.05104	0.03085	0.01201	0.00726	0.19682	0.11898
C31	−0.1047	0.06052	−0.0246	0.01424	−0.4038	0.23338

(b)

Atom number	M	M^-	M^+	f_k^+	f_k^-	f_k^0	s_k^+	s_k^-	s_k^0	ω_k^+	ω_k^-	ω_k^0
C1	−0.1023	−0.0925	−0.0086	−0.0098	0.09366	0.08389	−0.0023	0.02203	0.01974	−0.0377	0.36116	0.3235
C2	0.01541	−0.0766	0.00648	0.09201	−0.0089	0.08308	0.02165	−0.0021	0.01955	0.35482	−0.0344	0.32039
C3	−0.171	−0.1801	−0.1926	0.0091	−0.0217	−0.0126	0.00214	−0.0051	−0.003	0.03511	−0.0835	−0.0484
C4	0.29134	0.20787	0.22905	0.08347	−0.0623	0.02118	0.01964	−0.0147	0.00498	0.32189	−0.2402	0.08169
C5	−0.1988	−0.1379	−0.1236	−0.0609	0.07519	0.01429	−0.0143	0.01769	0.00336	−0.2348	0.28995	0.05512
C6	0.31443	0.18389	0.2206	0.13054	−0.0938	0.03671	0.03071	−0.0221	0.00864	0.5034	−0.3618	0.14157
C7	0.36424	0.26612	0.3463	0.09812	−0.0179	0.08019	0.02309	−0.0042	0.01887	0.37838	−0.0692	0.30921
C8	0.21434	0.15357	0.23516	0.06077	0.02083	0.0816	0.0143	0.0049	0.0192	0.23433	0.08032	0.31465
C9	0.01435	0.02251	0.13566	−0.0082	0.12131	0.11315	−0.0019	0.02854	0.02662	−0.0314	0.46778	0.43634
O10	−0.3576	−0.3513	−0.2938	−0.0063	0.06379	0.05753	−0.0015	0.01501	0.01354	−0.0242	0.246	0.22185
O11	−0.4282	−0.4309	−0.2719	0.00268	0.15627	0.15895	0.00063	0.03677	0.0374	0.01032	0.60263	0.61295
O12	−0.2842	−0.3904	−0.3292	0.10616	−0.045	0.06119	0.02498	−0.0106	0.0144	0.40939	−0.1734	0.23595
C13	−0.1414	−0.1257	−0.1241	−0.0157	0.01735	0.00163	−0.0037	0.00408	0.00038	−0.0606	0.06689	0.00628
C14	−0.039	−0.0665	−0.017	0.02752	0.02195	0.04947	0.00648	0.00516	0.01164	0.10614	0.08463	0.19077
C15	−0.1101	−0.1143	−0.0882	0.00421	0.02187	0.02608	0.00099	0.00515	0.00614	0.01623	0.08434	0.10057
C16	−0.0675	−0.1286	−0.0411	0.06111	0.02641	0.08752	0.01438	0.00621	0.02059	0.23566	0.10185	0.33751
C17	−0.1018	−0.1082	−0.0846	0.00646	0.01716	0.02362	0.00152	0.00404	0.00556	0.02491	0.06616	0.09107
C18	−0.0203	−0.0643	−0.0101	0.044	0.01018	0.05418	0.01035	0.0024	0.01275	0.16969	0.03926	0.20895
H19	0.17629	0.09163	0.14199	0.08465	−0.0343	0.05035	0.01992	−0.0081	0.01185	0.32644	−0.1323	0.19418
H20	0.0974	0.05258	0.13397	0.04482	0.03657	0.08139	0.01055	0.0086	0.01915	0.17285	0.14101	0.31386
H21	0.09873	0.04495	0.13962	0.05377	0.0409	0.09467	0.01265	0.00962	0.02227	0.20735	0.15772	0.36507
H22	0.09777	0.05104	0.13087	0.04674	0.0331	0.07984	0.011	0.00779	0.01878	0.18022	0.12764	0.30787
H23	0.10521	0.07289	0.12009	0.03232	0.01489	0.04721	0.0076	0.0035	0.01111	0.12464	0.0574	0.18204
C24	−0.109	−0.0952	−0.0492	−0.0138	0.05979	0.04603	−0.0032	0.01407	0.01083	−0.053	0.23054	0.1775
C25	0.08553	0.03449	0.11639	0.05104	0.03085	0.08189	0.01201	0.00726	0.01927	0.19682	0.11898	0.3158
O26	−0.3851	−0.2927	−0.2394	−0.0924	0.1457	0.05331	−0.0217	0.03428	0.01254	−0.3563	0.56187	0.20559
H27	0.12614	0.07306	0.15104	0.05309	0.0249	0.07799	0.01249	0.00586	0.01835	0.20471	0.09602	0.30074
H28	0.12425	0.06315	0.15403	0.06109	0.02978	0.09088	0.01437	0.00701	0.02138	0.23559	0.11485	0.35044
H29	0.12266	0.08408	0.13502	0.03858	0.01236	0.05093	0.00908	0.00291	0.01198	0.14876	0.04765	0.1964
H30	0.1577	0.07866	0.16266	0.07904	0.00496	0.084	0.0186	0.00117	0.01976	0.3048	0.01914	0.32394
C31	−0.202	−0.0973	−0.1414	−0.1047	0.06052	−0.0442	−0.0246	0.01424	−0.0104	−0.4038	0.23338	−0.1704
H32	0.07267	0.07634	0.15422	−0.0037	0.08155	0.07788	−0.0009	0.01919	0.01832	−0.0142	0.31449	0.30033
H33	0.18683	0.12381	0.17165	0.06302	−0.0152	0.04784	0.01483	−0.0036	0.01126	0.24303	−0.0585	0.18449
H34	0.05282	0.07183	0.1301	−0.019	0.07728	0.05826	−0.0045	0.01818	0.01371	−0.0733	0.29799	0.22467

Table 8: Polarizability and hyperpolarizability of Karanjin.

Polarizability	Values	Hyperpolarizability	Values
α_{XX}	−109.2190	β_{XXX}	22.0796
α_{XY}	3.9546	β_{XXY}	−8.6890
α_{YY}	−121.6217	β_{XYY}	−2.3092
α_{YZ}	1.5294	β_{YYY}	−61.3104
α_{ZZ}	−127.8736	β_{XXZ}	−8.1237
α_{XZ}	0.5918	β_{XYZ}	1.2207
$< \alpha >$	119.5714	β_{YYZ}	22.2892
—	—	β_{XZZ}	1.4229
—	—	β_{YZZ}	11.6211
—	—	β_{ZZZ}	0.2894
—	—	β_{Total}	63.6404

Table 9: Calculated thermodynamic properties of Karanjin by B3LYP/6-311G (d, p) methods.

	E (thermal) (kcalmol^{-1})	CV (cal K^{-1}mol^{-1})	S (cal K^{-1}mol^{-1})
Total	**171.700**	**67.244**	**133.534**
Translational	0.889	2.981	42.913
Rotational	0.889	2.981	34.406
Vibrational	169.922	61.283	56.215

C2 indicate that this site is prone to nucleophilic attack, while, for electrophilic attack, C31 and C24 are found to be the most active sites.

In pentagonal ring A, carbon is replaced by oxygen which has the most electronegative lone pair antibonding electron which extracts electrons from the neighboring carbon having the positive charge. To cancel this positive charge, it attracts the electron from C24 carbon. So C24 provides a better electrophilic site for the soft receptors. In hexagonal ring C, a carbon is replaced by oxygen having two lone pair antibonding electrons. Due to the repulsion of these antibonding electrons, the shape of the ring gets distorted. Ring C has two substituent groups at para and meta positions. At meta position, oxygen is attached to the ring C and at para position O–CH_3 group is attached. Oxygen is more electronegative than carbon which extracts electron from carbon. Due to this reason, C31 carbon atom of methyl group is a better center for electrophilic substitution. In hexagonal ring C, electron withdrawing group O–CH_3 extracts electron from C9 atom of the ring C to fulfill the deficiency; C9 atom extracts electron from C7 atom and hence because of the C7 atom being electron deficient it extracts electron from O11 so C7 atom becomes a potential site for a nucleophilic attack.

4.11. Dipole Moment, Polarizability, Hyperpolarizability, and Thermodynamic Properties. Dipole moment (μ), polarizability $\langle\alpha\rangle$, and total first static hyperpolarizability β [41, 42] are also calculated (in Tables 5 and 8) by using density functional theory. They can be expressed in terms of x, y, and z components and are given by following (4):

$$\mu = \left(\mu_x^2 + \mu_y^2 + \mu_z^2\right)^{1/2}$$

$$\langle\alpha\rangle = \frac{1}{3}\left[\alpha_{xx} + \alpha_{yy} + \alpha_{zz}\right]$$

$$\begin{aligned}\beta_{\text{Total}} &= \left(\beta_x^2 + \beta_y^2 + \beta_z^2\right)^{1/2} \\ &= \left[\left(\beta_{xxx} + \beta_{xyy} + \beta_{xzz}\right)^2 \right. \\ &\quad + \left(\beta_{yyy} + \beta_{yxx} + \beta_{yzz}\right)^2 \\ &\quad \left. + \left(\beta_{zzz} + \beta_{zxx} + \beta_{zyy}\right)^2\right]^{1/2}.\end{aligned} \tag{4}$$

The β components of Gaussian output are reported in atomic units, where 1 a.u. = 8.3693×10^{-33} e.s.u. For Karanjin, the calculated dipole moment value is 3.86 Debye. Having higher dipole moment than water (2.16 Debye), "Karanjin" can be used as better solvent. We see a greater contribution of α_{zz} in molecule which shows that the molecule is elongated more towards Z direction and is more contracted to X direction. Perpendicular part contributes with a less part of polarizability of molecule. B_{yyy} and β_{yyz} contribute with a larger part of hyperpolarizability in the molecule. This shows that YZ plane and Y-axis are more optically active in these directions. Standard thermodynamic functions such as free energy, constant volume heat capacity CV, and entropy S have also been calculated for "Karanjin" and are given in Table 9. These functions can provide helpful information for further study of the title compounds.

5. Conclusion

In this work, the compound "Karanjin" an anti-HIV drug was experimentally isolated and identified and its bioactivity along with detailed quantum chemical studies was carried out. The optimized geometry of the "Karanjin" molecule has been determined by the method of density functional

theory (DFT). For both geometry and total energy, it has been combined with B3LYP functional having 6-311 g (d, p) as the basis set. Using this optimized structure, we have calculated the infrared wavenumbers and compared them with the experimental data. The calculated wavenumbers are in an excellent agreement with the experimental values. On the basis of fully optimized ground-state structure, TDDFT//B3LYP/LANL2DZ calculations have been used to determine the low-lying excited states of "Karanjin." Reactivity reflects the susceptibility of a substance towards a specific chemical reaction and plays a key role in, for example, the design of new molecules and understanding biological systems and material science. Hyperpolarizability is mainly controlled by the planarity of the molecules, the donor and accepter strength, and bond length alteration. The values of hyperpolarizability indicate a possible use of these compounds in electrooptical applications. We have also discussed global and local reactivity descriptors sites for both molecules during electrophilic, nucleophilic, and radical attacks. These values represent the qualitative descriptors of reactivity of different atoms in the molecule. This compound shows anti-HIV activity so these theoretical and experimental aspects can provide a path for researchers in future.

Conflict of Interests

The authors of the paper have no conflict of interests in the present work.

Acknowledgment

The corresponding author Apoorva Dwivedi is grateful to Professor Neeraj Misra for providing valuable suggestions.

References

[1] *The Wealth of India—A Dictionary of Indian Raw Materials*, vol. 8, Council of Scientific and Industrial Research, New Delhi, India, 2005.

[2] K. R. Kirtikar and B. D. Basu, *Indian Medicinal Plants*, vol. 1, 2nd edition, 1981.

[3] S. A. Dahanukar, R. A. Kulkarni, and N. N. Rege, "Pharmacology of medicinal plants and natural products," *Indian Journal of Pharmacology*, vol. 32, no. 4, pp. S81–S118, 2000.

[4] G. P. Garg, "A new component from leaves of Pongamia glabra," *Planta Medica*, vol. 39, no. 1, pp. 73–74, 1979.

[5] S. B. Malik, T. R. Seshadri, and P. Sharma, "Minort components of the leaves of pongamia glabra," *Indian Journal of Chemistry*, vol. 14, pp. 229–230, 1976.

[6] P. Sharma, T. R. Seshadri, and S. K. Mukerjee, "Some synthesis and natural analogues of globrachromene," *Indian Journal of Chemistry*, vol. 11, pp. 98/5–98/6, 1973.

[7] S. Rangaswamy and T. R. Seshadri, "Extraction and recovery of karanjin: a value addition to karanja (Pongamia pinnata) seed oil," *Indian Journal of Pharmacology*, vol. 3, p. 3, 1941.

[8] B. S. Parmar and K. C. Gulati, "Synergists for pyrethrins (II)-karanjin," *Indian Journal of Entomology*, vol. 31, pp. 239–243, 1969.

[9] W. E. Sapna, T. C. Sindhu Kanya, A. M. Mamatha et al., "Karanjin, a flavonoid inhibits lipoxygenases," in *Proceedings of National Academy of Science India*, CFTRI, Mysore, India, 2007.

[10] P. Hohenberg and W. Kohn, "Inhomogeneous electron gas," *Physical Review*, vol. 136, no. 3B, pp. B864–B871, 1964.

[11] A. D. Becke, "Density-functional thermochemistry. III. The role of exact exchange," *The Journal of Chemical Physics*, vol. 98, no. 7, pp. 5648–5652, 1993.

[12] C. Lee, W. Yang, and R. G. Parr, "Development of the Colle-Salvetti correlation-energy formula into a functional of the electron density," *Physical Review B*, vol. 37, no. 2, pp. 785–789, 1988.

[13] M. J. Frisch, G. W. Trucks, H. B. Schlegel et al., *Gaussian 09*, Gaussian, Pittsburgh, Pa, USA, 2009.

[14] P. L. Fast, J. Corchado, M. L. Sanches, and D. G. Truhlar, "Optimized parameters for scaling correlation energy," *The Journal of Physical Chemistry A*, vol. 103, pp. 3139–3143, 1999.

[15] A. Frisch, A. B. Nelson, and A. J. Holder, "Gauss View," Pittsburgh, Pa, USA, 2005.

[16] V. Vismaya, S. M. Belagihally, S. Rajashekhar, V. B. Jayaram, S. M. Dharmesh, and S. K. C. Thirumakudalu, "Gastroprotective properties of karanjin from Karanja (Pongamia pinnata) seeds; Role as antioxidant and H+, K+-ATPase inhibitor," *Evidence-based Complementary and Alternative Medicine*, vol. 2011, Article ID 747246, 10 pages, 2011.

[17] S. Sharma, M. Verma, R. Prasad, and D. Yadav, "Efficacy of non-edible oil seedcakes against termite (Odontotermes obesus)," *Journal of Scientific and Industrial Research*, vol. 70, no. 12, pp. 1037–1041, 2011.

[18] R. Ranga Rao, A. K. Tiwari, P. Prabhakar Reddy et al., "New furanoflavanoids, intestinal α-glucosidase inhibitory and free-radical (DPPH) scavenging, activity from antihyperglycemic root extract of Derris indica (Lam.)," *Bioorganic and Medicinal Chemistry*, vol. 17, no. 14, pp. 5170–5175, 2009.

[19] V. Vismaya, W. Sapna Eipeson, J. R. Manjunatha, P. Srinivas, and T. C. Sindhu Kanya, "Extraction and recovery of karanjin: a value addition to karanja (Pongamia pinnata) seed oil," *Industrial Crops and Products*, vol. 32, no. 2, pp. 118–122, 2010.

[20] J.-H. Wang, S.-C. Tam, H. Huang, D.-Y. Ouyang, Y.-Y. Wang, and Y.-T. Zheng, "Site-directed PEGylation of trichosanthin retained its anti-HIV activity with reduced potency in vitro," *Biochemical and Biophysical Research Communications*, vol. 317, no. 4, pp. 965–971, 2004.

[21] D. Sajan, H. J. Ravindra, N. Misra, and I. H. Joe, "Intramolecular charge transfer and hydrogen bonding interactions of nonlinear optical material N-benzoyl glycine: vibrational spectral study," *Vibrational Spectroscopy*, vol. 54, no. 1, pp. 72–80, 2010.

[22] V. Mukherjee, N. P. Singh, and R. A. Yadav, "FTIR and Raman spectra, DFT and SQMFF calculations for geometrical interpretation and vibrational analysis of some trifluorobenzoic acid dimers," *Vibrational Spectroscopy*, vol. 52, no. 2, pp. 163–172, 2010.

[23] M. Hariharan and S. S. Rajan, "Crystal structure communications," *Acta Crystallographica C*, vol. 46, pp. 437–439, 1990.

[24] M. Alcolea Palafox, G. Tardajos, A. Guerrero-Martínez et al., "FT-IR, FT-Raman spectra, density functional computations of the vibrational spectra and molecular geometry of biomolecule 5-aminouracil," *Chemical Physics*, vol. 340, no. 1-3, pp. 17–31, 2007.

[25] J. S. Singh, "FTIR and Raman spectra and fundamental frequencies of biomolecule: 5-Methyluracil (thymine)," *Journal of Molecular Structure*, vol. 876, no. 1–3, pp. 127–133, 2008.

[26] C. P. Beetz Jr. and G. Ascarelli, "The low frequency vibrations of pyrimidine and purine bases," *Spectrochimica Acta A: Molecular Spectroscopy*, vol. 36, no. 3, pp. 299–313, 1980.

[27] J. Bandekar and G. Zundel, "The role of CO transition dipole-dipole coupling interaction in uracil," *Spectrochimica Acta A: Molecular Spectroscopy*, vol. 39, no. 4, pp. 337–341, 1983.

[28] K.-C. Chou, "Biological functions of low-frequency vibrations (phonons). III. Helical structures and microenvironment," *Biophysical Journal*, vol. 45, no. 5, pp. 881–889, 1984.

[29] H. Frohlich, *Biological Coherence and Response to External Stimuli*, Springer, Berlin, Germany, 1988.

[30] D. F. V. Lewis, C. Loannides, and D. V. Parkee, "Interaction of a series of nitriles with the alcohol-inducible isoform of P450: computer analysis of structure-activity relationships," *Xenobiotica*, vol. 24, pp. 401–408, 1984.

[31] Z. Zhou and R. G. Parr, "Activation hardness: new index for describing the orientation of electrophilic aromatic substitution," *Journal of the American Chemical Society*, vol. 112, no. 15, pp. 5720–5724, 1990.

[32] I. Fleming, *Frontier Orbitals and Organic Chemical Reactions*, John Wiley & Sons, New York, NY, USA, 1976.

[33] M. Bohl, K. Ponsold, and G. Reck, "Quantitative structure-activity relationships of cardiotonic steroids using empirical molecular electrostatic potentials and semiempirical molecular orbital calculations," *Journal of Steroid Biochemistry*, vol. 21, no. 4, pp. 373–379, 1984.

[34] D. F. Lewis and V. Griffiths, "Molecular electrostatic potential energies and methylation of DNA bases: a molecular orbital-generated quantitative structure-activity relationship," *Xenoviotica*, vol. 17, pp. 769–776, 1987.

[35] A. Kumar and P. C. Mishra, "Structure-activity relationships for some anti-HIV drugs using electric field mapping," *Journal of Molecular Structure*, vol. 277, pp. 299–312, 1992.

[36] R. G. Pearson, "Absolute electronegativity and hardness: applications to organic chemistry," *Journal of Organic Chemistry*, vol. 54, no. 6, pp. 1423–1430, 1989.

[37] R. G. Parr, L. V. Szentpály, and S. Liu, "Electrophilicity Index," *Journal of the American Chemical Society*, vol. 121, pp. 1922–1924, 1999.

[38] P. K. Chattaraj and S. Giri, "Stability, reactivity, and aromaticity of compounds of a multivalent superatom," *Journal of Physical Chemistry A*, vol. 111, no. 43, pp. 11116–11121, 2007.

[39] J. Padmanabhan, R. Parthasarathi, V. Subramanian, and P. K. Chattaraj, "Electrophilicity-based charge transfer descriptor," *Journal of Physical Chemistry A*, vol. 111, no. 7, pp. 1358–1361, 2007.

[40] P. W. Ayers and R. G. Parr, "Variational principles for describing chemical reactions: the Fukui function and chemical hardness revisited," *Journal of the American Chemical Society*, vol. 122, no. 9, pp. 2010–2018, 2000.

[41] D. A. Kleinman, "Nonlinear dielectric polarization in optical media," *Physical Review B*, vol. 126, no. 6, pp. 1977–1979, 1962.

[42] J. Pipek and P. G. Mezey, "A fast intrinsic localization procedure applicable for ab initio and semiempirical linear combination of atomic orbital wave functions," *The Journal of Chemical Physics*, vol. 90, no. 9, pp. 4916–4926, 1989.